PROGRESS IN PHOTOVOLTAICS: RESEARCH AND APPLICATIONS
Prog. Photovolt: Res. Appl. (in press)
Published online in Wiley InterScience (www.interscience.wiley.com) DOI: 10.1002/pip.768

Research

Fabrication of Screen-Printing Pastes From TiO_2 Powders for Dye-Sensitised Solar Cells

Seigo Ito, Peter Chen, Pascal Comte, Mohammad Khaja Nazeeruddin, Paul Liska, Péter Péchy and Michael Grätzel*†
Laboratory of Photonique and Interfaces (LPI), Institute des Sciences et Ingenierie Chimiques (ISIC), École Polytechnique Fédérale de Lausanne (EPFL), CH-1015 Lausanne, Switzerland

A preparation technique of TiO_2 screen-printing pastes from commercially-available powders has been disclosed in order to fabricate the nanocrystalline layers without cracking and peeling-off over 17 μm thickness for the photoactive electrodes of the dye-sensitised solar cells. A conversion efficiency of 8·7% was obtained by using a single-layer of a semi-transparent-TiO_2 film. A conversion efficiency of 9·2% was obtained by using double-layers composed of transparent and light-scattering TiO_2 films for a photon-trapping system. Copyright © 2007 John Wiley & Sons, Ltd.

KEY WORDS: titanium dioxide; nanocrystalline electrode; dye-sensitised solar cells

Received 9 January 2007; Revised 20 March 2007

INTRODUCTION

Dye-sensitised solar cells (DSCs) are currently attracting academic and commercial interest as regenerative low-cost alternatives to conventional solid state devices.[1,2] So far, the best performing nanocrystalline-TiO_2 electrodes have been fabricated by hydrothermal autoclaving and screen-printing deposition.[3–5] Screen-printing of TiO_2 is a widespread industrially-applied method because of the fast-printing technique and of the coating facility with fine controlling of the position and thickness. Other applied fields are gas sensors (humidity, O_2, H_2, NO_X, CH_X, CO, etc.), ion sensors, piezoelectric devices, microfiltration membranes, Gamma-radiation sensors, electroluminescent devises, electrochromic display, antireflection coatings on silicon solar cells, microwave applications, photocatalyst coatings and so on. The nontoxicity of titanium dioxide, which is used in paints, cosmetics and health care products, adds advantages to the fields.

The key point on the screen-printing is the quality and characteristics of TiO_2 paste. For the best-performing TiO_2 electrodes, the synthesis of TiO_2 paste involves hydrolysis of $Ti(OCH(CH_3)_2)_4$ in water at 250°C (70 atms) for 12 h, followed by conversion of the water to ethanol by three-times centrifugation. Finally, the ethanol is exchanged with α-terpineol by sonication and evaporation.[3] Totally, it takes 3 days. Such a long-time procedure of TiO_2 pastes is economically unsuitable for industrial production and has to be reduced. Towards this goal, several reports were published in order to fabricate screen-printing paste from a commercially-available TiO_2 powder (P25, Degussa).[6–9] Most of the pastes were based on water and alcohols, which induce TiO_2 aggregation and yielding poorly reproducible results in long-term experiments. On the other hand, α-terpineol-based

* Correspondence to: Michael Grätzel, Laboratory of Photonique and Interfaces (LPI), Institute des Sciences et Ingenierie Chimiques (ISIC), École Polytechnique Fédérale de Lausanne (EPFL), CH-1015 Lausanne, Switzerland.
†E-mail: michael.graetzel@epfl.ch

pastes[3–5] are very stable at long-term and give very reproducible results for several years. However, a reported paste made from P25 and α-terpineol did not give better DSCs than that of a water-based paste.[9]

In this study, we have developed a new procedure which takes only 4 h to produce TiO_2 pastes with α-terpineol from commercially-available powders, resulting in DSCs with *ca*. 9% conversion efficiencies. Moreover, the most important point of this work is to utilise the commercially-available TiO_2 particles for the high-efficiency DSCs, because the synthesis of the homemade TiO_2 particle demands the delicate techniques and consequently the different batch of TiO_2 particle might give different results. For the reproducible results, therefore, it is important to investigate a new fabrication method of TiO_2 paste from commercially-available particles. This report will be of great help for the people who are engaged with DSCs.

EXPERIMENTAL

Materials

Three kinds of commercially-available TiO_2 powders were used: P25 (av. 30 nm by Brunauer-Emmett-Teller (BET), 80% anatase ($d = 21$ nm) and 20% rutile ($d = 50$ nm), via $TiCl_4$-fumed gas synthesis, Degussa, Germany); ST21 (av. 25 nm by BET, 100% anatase, via sulfuric-acid synthesis, Ishihara Sangyo, Japan); ST41 (av. 160 nm by BET, 100% anatase, via sulfuric-acid synthesis, Ishihara Sangyo, Japan). Two kinds of pure powders of ethyl celluloses (5–15 mPas at 5% in toluene:ethanol/80:20 at 25 oC, #46 070, Fluka; 30–50 mPas at 5% in toluene:ethanol/80:20 at 25°C, #46 080, Fluka) were dissolved beforehand in an ethanol solution (these powders of ethyl cellulose don't contain toluene and ethanol which were mixed with ethyl cellulose just to show the specification results of viscosity). Each concentration of the ethyl cellulose was 5 wt%: the total amount of ethyl celluloses was 10 wt% in ethanol.

4-*tert*-butylpyridine (Aldrich), acetonitrile (Fluka) and valeronitrile (Fluka) were purified by vacuum distillation. Guanidinium thiocyanate (Aldrich) and H_2PtCl_6 (Fluka) were used as received. H_2O was purified by distillation and filtration (Milli-Q). $TiCl_4$ (Fluka) was diluted with water to 2 M at 0°C to make a stock solution, which was kept in a freezer and freshly diluted to 40 mm with water for each $TiCl_4$ treatment of the F-doped tin oxide (FTO) coated glass plates. Iodine (99·999%, Superpur®, Merck) was used as received. The synthesis of *cis*-di(thiocyanato)-*N,N'*-bis(2,2'-bipyridyl-4-carboxylic acid-4'-tetrabutylammonium carboxy late) ruthenium (II) (**N-719**) and butylmethylimidazolium iodide (BMII) were reported in our previous paper.[10,11] The chromatographic purification of N-719 was carried out three times on a column of Sephadex LH-20 using the following procedure.[4,5]

Preparation of TiO_2 paste

The fabrication scheme for TiO_2 pastes was described in Figure 1. At each step, liquids were added drop by drop into an alumina mortar, which is more stable than a porcelain one. The diameter of the mortar was *ca*. 20 cm. The condition was in the ambient air at room temperature. The TiO_2 powders stuck on the inside of the mortar should be removed by a plastic spatula in order to grind large aggregates. The TiO_2 dispersions in the mortar were transferred with excess of ethanol (100 ml) to a tall beaker and stirred with a 4 cm long magnet tip at 300 rpm. The ultrasonic homogenisation was performed with using a Ti-horn-equipped sonicator (Vibra cell 72408, Bioblock scientific). Anhydrous terpineol (Fluka) and the mixture solution of two ethyl celluloses in ethanol were added, followed by stirring and sonication. The contents in dispersion were concentrated by evaporator at 35°C with 120 mbar at first. The pressure was evacuated until 10 mbar. The pastes were finalised with a three-roller-mill grinder (EXAKT).

In this scheme (Figure 1), the coexistence of water and acetic acid was important. We tried another combination with nitric acid, hydrochloric acid, acetyl acetone, polyethylene glycol, triton X-100 and so on. Without water and/or acetic acid, however, the porous-TiO_2 layers over 10 μm thickness were mechanically unstable and did not keep the structure after sintering due to the large cracks and peeling-up from substrate.

DOI: 10.1002/pip

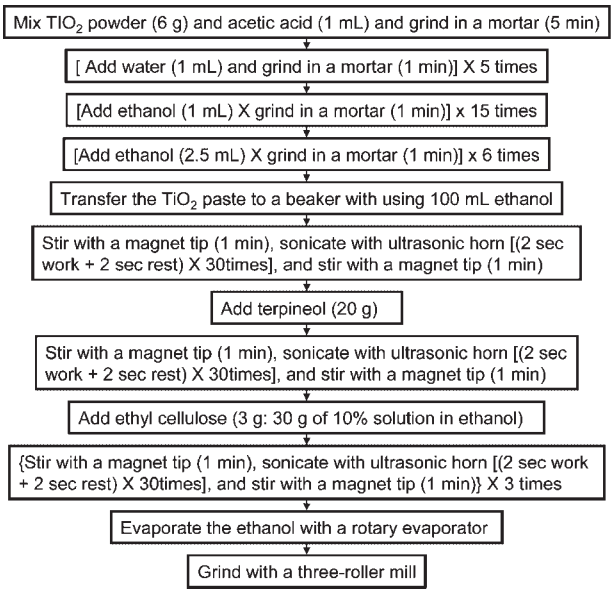

Figure 1. Fabrication scheme of screen-printing paste from a nanocrystalline-TiO_2 powder

We speculate the reason as below. In order to make a good connection between TiO_2 particles and between a TiO_2 particle and SnO_2 surface, hydroxides (–OH) have to be on the surface and make strong chemical bonding between each other by dehydration at sintering:

$$M_1{-}OH + HO - M_2 \rightarrow M_1{-}O - M_2 + H_2O$$

where, M_1 shows a titanium atom on a surface of a particle and M_2 shows a titanium atom of another particle or a tin atom on a plate of transparent conductive oxide (TCO) substrate (F-doped tin oxide (FTO) glass). The water added at first can make the surface covered by hydroxides. At the same time, each particle has to be isolated from each other and not to be aggregated. The aggregates in matrix can make large shrinkage of the film at the sintering, resulting in the peering-off from the TCO substrate. The acetic acid can be adsorbed on the surface of TiO_2 and prohibits each particle from the aggregation. At the same time, the proton (H^+) of acid can also be adsorbed on the surface and shifts the Zeta potential to positive, resulting in repelling the particles from each other.

About the reproducibility, as long as the timing of adding, mixing and grinding the materials in the mortar is kept up, the result is quite reproducible (the data was not shown). However, by changing the timing, it can change. For example, if we add all of the ethanol in one time, it is very difficult to remove the aggregate. The paste can be a film peeled-off from the substrate or be a DSC electrode with a low photovoltaic efficiency.

Preparation of nanocrystalline-TiO_2 electrodes

To prepare the DSC working electrodes, the FTO glass used as current collector (Solar 4 mm thickness, 10 $\Omega/\square$, Nippon Sheet Glass, Japan) was first cleaned in a detergent solution using an ultrasonic bath for 15 min, and then rinsed with water and ethanol. After treatment in a UV-O_3 system (Model No. 256–220, Jelight Company, Inc.) for 18 min, the FTO glass plates were immersed into a 40 mm aqueous $TiCl_4$ aqueous solution at 70°C for 30 min and washed with water and ethanol. A layer of paste was coated on the FTO glass plates by screen-printing (90T, Estal Mono, Schweiz. Seidengazefabrik AG Thal), kept in a clean box for 3 min with ethanol so that the paste can relax to reduce the surface irregularity and then dried for 6 min at 125°C. The screen characteristics are as

DOI: 10.1002/pip

follows: material, polyester; mesh count, 90T mesh/cm (or 230T mesh/inch); mesh opening, 60 μm; thread diameter, 50 μm; open surface, 29·8%; fabric thickness, 83 μm; theoretical paste volume, 24·5 $cm^3\,m^{-2}$; K/KS volume, 17·0 $cm^3\,m^{-2}$; weight, 48 $g\,m^{-2}$. This screen-printing procedure (with coating, storing and drying) was repeated to change the thickness of the nanocrystalline-TiO_2 working electrode. For the single-layer electrode, the TiO_2 paste of ST21 was used, resulting in a light-scattering film. For the double-layer electrode, the paste of P25 for the transparent layer was coated by screen-printing and dried at 125°C, and then, the second layers of ST41 for the light-scattering layer were deposited by screen-printing to 4–5 μm thickness. The electrodes coated with the TiO_2 pastes were gradually heated under an airflow at 325°C for 5 min, at 375°C for 5 min, at 450°C for 15 min and 500°C for 15 min°C. After sintering, the surface area of the TiO_2 electrodes was measured precisely by a scanner with 600 dpi resolution in grey mode, followed by integration of the resulting image.[4]

DSC assembling

After the size measurement, the TiO_2 film was treated with 40 mm $TiCl_4$ solution as described above, rinsed with water and ethanol and sintered at 500°C for 30 min. At 80°C in the cooling, the TiO_2 electrode was immersed into a 0·5 mM N-719 dye solution in a mixture of acetonitrile and *tert*-butyl alcohol (volume ratio: 1:1) and kept at room temperature for 20–24 h to complete the sensitiser uptake.

To prepare the counter electrode, a hole was drilled in the FTO glass (LOF Industries, TEC 15 Ω/□, 2·2 mm thickness) by sand blasting. The perforated sheet was washed with H_2O as well as with a 0·1 M HCl solution in ethanol and cleaned by ultrasound in an acetone bath for 10 min. After removing residual organic contaminants by heating in air for 15 min at 400°C, the Pt catalyst was deposited on the FTO glass by coating with a drop of H_2PtCl_6 solution (2 mg Pt in 1 ml ethanol) and repeating the heat treatment at 400°C for 15 min.

The dye-covered TiO_2 electrode and Pt-counter electrode were assembled into a sandwich type cell and sealed with a hot-melt gasket of 25 μm thickness made of the ionomer Surlyn 1702 (Dupont). The aperture of the Surlyn frame was 2 mm larger than that of the TiO_2 area and its width was 1 mm. A drop of the electrolyte, a solution 0·60 M BMII, 0·03 M I_2, 0·10 M guanidinium thiocyanate and 0·50 M 4-*tert*- butylpyridine in the mixture of acetonitrile and valeronitrile (volume ratio: 85:15)) was put on the hole in the back of the counter electrode. The electrolyte was introduced into the cell via vacuum backfilling. The cell was placed in a small vacuum chamber to remove inside air. Exposing it again to ambient pressure causes the electrolyte to be driven into the cell. Finally, the hole was sealed using a hot-smelt ionomer film (Bynel 4702, 35 μm thickness, Du-Pont) and a cover glass (0·1 mm thickness).

Photovoltaic measurement of DSC

Light reflection losses were eliminated using a self-adhesive fluorinated polymer film (ARKTOP, ASAHI GLASS) that served at the same time as a 380 nm UV cut-off filter. Photovoltaic measurements employed an AM 1·5 solar simulator. The power of the simulated light was calibrated to be 100 mW cm^{-2} by using a reference Si photodiode equipped with an IR-cutoff filter (KG-3, Schott), which was calibrated at three solar-energy institutes (ISE (Germany), NREL (USA), SRI (Switzerland)).[4] I-V curves were obtained by applying an external bias to the cell and measuring the generated photocurrent with a Keithley model 2400 digital source meter. The voltage step and delay time of photocurrent were 10 MV and 40 ms, respectively.

RESULTS AND DISCUSSION

Morphology of screen-printed TiO_2 films

Figure 2 shows SEM pictures of porous TiO_2 films. We can notice that the particles of P25 contained small particles (anatase, 20 nm) and large particles (rutile, 40 nm). Compared with the pictures of TiO_2 films made via

DOI: 10.1002/pip

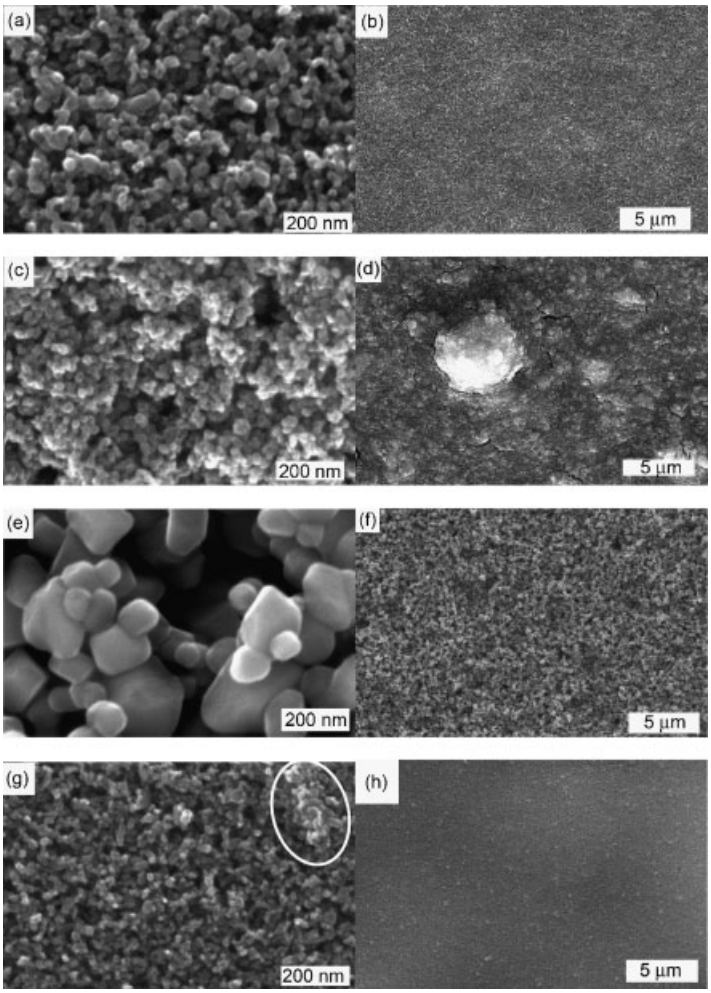

Figure 2. SEM photographs of porous TiO_2 films showing the surface morphology of P25 (a, b), ST21 (c, d), ST41 (e, f) and homemade TiO_2 ($d = 20$ nm) (g, h) with two types of magnification: 120000× (a, c, e, g) and 5000× (b, d, f, h)

colloidal synthetic routes (Figure 2g and h), the P25 film contained no aggregates (Figure 2a), and was dispersed homogeneously over the large area (Figure 2b). On the other hand, ST21 showed the small aggregates (*ca.* 100 nm, Figure 2c) and the large aggregates (micron-meter order, Figure 2d). The large aggregates of ST21 were very difficult to be broken by this procedure and gave small cracks in the porous TiO_2 layer (Figure 2d). The difference of the morphologies between P25 and ST21 was due to the synthesis method: fumed-$TiCl_4$ and sulphuric-acid routes, respectively. ST41 contained 50–200 nm large particles (Figure 2e). The average was 160 nm from BET data (measured by Ishihara Sangyo). Although ST41 also was made by the sulphuric-acid synthesis, this layer was homogeneous over the large area (Figure 2f). Hence, the aggregations between ST41 particles did not affect the surface morphology on a large scale. For the comparison with homemade TiO_2, we added the SEM pictures (Figure 2g and h). Although the aggregates about 200 nm existed (in a white circle of Figure 2g) and we can find small dots in Figure 2h from the aggregate, the surface was very smooth and uniform over the large area (Figure 2h).

Figure 3 shows cross sections of nanocrystalline-TiO_2 layers by surface-profiling method (Alphastep 550). Each layer was the single screen-printing using a 90T mesh. The layer of P25 and ST41 was relatively flat

DOI: 10.1002/pip

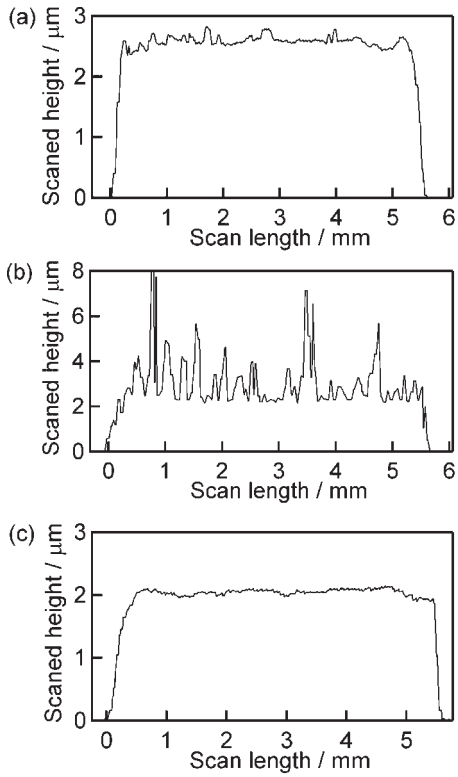

Figure 3. Cross sections of nanocrystalline-TiO_2 layers by surface-profiling method (Alfastep550): P25 (a), ST21 (b) and ST41 (c)

compared with that of ST21. This phenomenon reflected the morphology which was observed by SEM (Figure 2). The flatness of P25 and ST41 layers reflect the homogeneous dispersion of particles. On the other hand, the roughness of ST21 layer reflects the aggregations (Figure 2d).

Figure 4a shows the photograph of screen-printed layers with a background of garden plants. The P25 film was transparent and pale blue. We can see the clear image of the background. The ST21 film was semi-transparent and we can see slightly the images of background. The ST41 was opaque and completely white and we cannot see any images through the film. Figure 4b shows the transmittance spectra of screen-printed TiO_2 layers used in Figures 3 and 4a. The P25 layer transmitted 60% of incident light above 480 nm wavelength and diffused the shorter wavelength effectively. Therefore, the P25 layer was pale blue (Figure 4a). The transmittance of ST21 increased linearly from 378 to 820 nm wavelength, and the transmittance at 820 nm was half that of P25. ST41 blocked the incident light below 600 nm wavelength and let the incident light slightly through above that. For the comparison with homemade TiO_2, we added the data of transmission, which shows the higher transparency of the homemade TiO_2 layer than those of commercially-available TiO_2 powders. However, if 100%-anatase nanoparticles made by fumed-$TiCl_4$ synthesis is available, more highly-transparent TiO_2 layer can be fabricated.

It has been reported that particles over 100 nm can diffuse visible light effectively.[12–14] Hence, ST41 (av. 160 nm) was able to diffuse visible light. This is the reason why the layer of ST41 was white and opaque (Figure 4). On the other hand, the particle sizes of P25 (av. 21 nm) and ST41 (av. 20 nm) were close. Hence, the optical difference between layers of P25 (transparent) and ST21 (hazy) (Figure 4) arises from the aggregates and the roughness, acting as light-scattering centres (Figures 2 and 3). The difference of morphologies was due to the synthetic variation: a liquid-phase synthesis for ST21 and a gas-fumed synthesis for P25.

DOI: 10.1002/pip

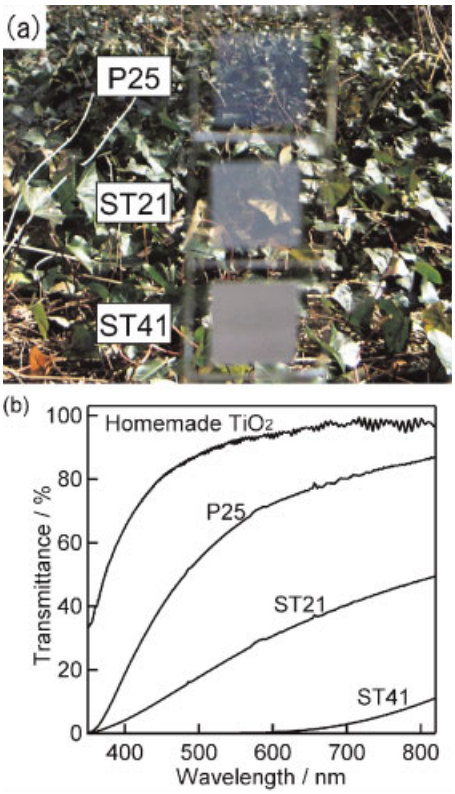

Figure 4. A picture (a) and transmittance spectra (b) of screen-printed nanocrystalline-TiO_2 layers. The transmittance measurements were performed with cover glass plates which were attached on the surface of TiO_2 layer, and the pores in nanocrystalline-TiO_2 layers were filled with butoxyacetonitrile to decrease the light-scattering effect. The optical background for (b) was obtained by using the same FTO/glass substrate, butoxyacetonitrile and the cover glass plate

DSC Photovoltaics related with thickness of nanocrystalline-TiO_2 electrodes

In order to fabricate DSCs, the TiO_2 pastes were coated by screen-printing on FTO/glass substrates and assembled to DSC. For the high-efficiency DSC, therefore, we applied P25 and ST41 to transparent and light-scattering layers in double-layer photon-trapping system as reported, respectively.[3–5] Since the ST21 layer was semi-transparent, we cannot expect the optical merit for applying the ST21 layer to the double-layer photon-trapping system. Therefore, the ST21 layer was used in DSC electrodes as a single layer.

Figure 5 shows the relationships between the screen-printing times and the thickness of nanocrystalline-TiO_2 (P25 and ST21) layers, which were used for DSC electrodes (Figures 5 and 6). The 'P25 + ST41' and 'ST21' layers were double-layer and single-layer structures, respectively, as written in the previous paragraph. The thickness of ST41 was fixed at 5·7 μm, which was obtained by the interception of *y*-axis. The linear relationship between the coating time and the thickness was confirmed. The thicknesses of one screen-print coating of P25 and ST21 were obtained as 1·9 μm and 2·0 μm, respectively. Each paste gave a thick layer over 17 μm without cracking and peeling-up at the exterior; nanoscale cracks in the ST21 layer were observed by SEM (see Figure 2d).

Figure 6 shows the photovoltaic-characteristic variations of open-circuit photo voltage (a, V_{OC}), short-circuit photo current density (b, J_{SC}), fill factor (c, FF) and conversion efficiency (d, η). The V_{OC} and FF decreased linearly with increasing thickness, but the changing ratios were just 10% and 2%, respectively (Figure 6a and c). On the other hand, J_{SC} of P25-ST41 and ST21 increased by 30% and 50%, respectively (Figure 6b), which

DOI: 10.1002/pip

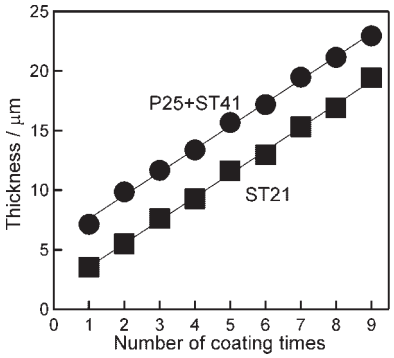

Figure 5. Relationship between number of coating times and thickness of screen-printed nanocrystalline-TiO_2 layers of P25 + ST41 and ST21. In P25 + ST41, the thickness of P25 was varied and that of ST41 was fixed at 5·7 μm by two-times screen printing for utilisation of photovoltaic measurements in Figures 6 and 7

projects the variation of η (Figure 6d). Resulting efficiencies of double-layer (P25-ST41) and single-layer (ST21) electrodes had peaks at 14 and 17 μm thickness of nanocrystalline layers (P25 and ST21), respectively (Figure 6d). Figure 7 shows photo I-V curves of best efficiency DSCs using P25-ST41 and ST21. The photovoltaic characteristics were $J_{SC} = 16{\cdot}25\,mA\,cm^{-2}$, $V_{OC} = 779\,mV$, $FF = 0{\cdot}730$, and $\eta = 9{\cdot}24\%$ with P25-ST41 and $J_{SC} = 15{\cdot}3\,mA\,cm^{-2}$, $V_{OC} = 778\,mV$, $FF = 0{\cdot}733$, and $\eta = 8{\cdot}75\%$ with ST21. These efficiencies are the best results published ever with using commercially-available TiO_2 powders.

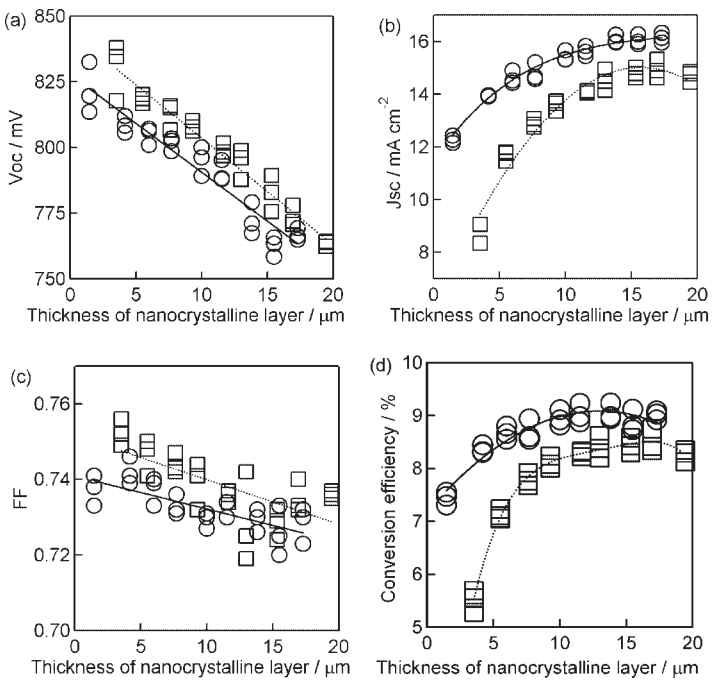

Figure 6. Photovoltaic-characteristics relationship with nanocrystalline (P25 and ST21)-layer thickness of P25 + ST41 (○) and ST21 (□) electrodes: V_{OC} (a), J_{SC} (b), FF (c) and conversion efficiency (η) (d). The thickness of ST41 was fixed at 5·7 μm for the light-scattering layer. The solid and doted lines were fitted to the average data of P25 + ST41 and ST21, respectively

DOI: 10.1002/pip

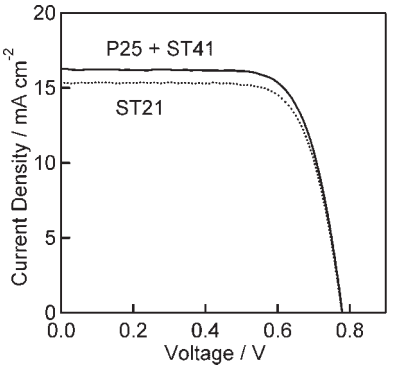

Figure 7. Photo I-V curves of best-efficiency dye-sensitised solar cells using nanocrystalline-TiO_2 electrodes fabricated from commercially-available nanocrystalline-TiO_2 powders (P25 + ST41, $\eta = 9{\cdot}24\%$; ST21, $\eta = 8{\cdot}75\%$) under 100 mW cm^{-2} AM 1·5 irradiation

CONCLUSION

In summary, this screen-printing technique enabled the fabrication of nanocrystalline layers over 17 μm thickness from commercially-available TiO_2 powders. The result of 9·2% efficiency was lower than that from our homemade double-layered electrode (10–11%).[4,5] However, this report shows the best efficiencies using commercially-available TiO_2 powders, which is very important for the world-wide market production of solar cells.

Since P25 and ST21 contained rutile particles and large aggregates, respectively, the efficiencies were lower than 10%. If we can get more transparent electrodes using 100%-anatase nanoparticles made by fumed-$TiCl_4$ synthesis, more highly efficient photovoltaic DSC can be fabricated.

We believe that this report can be of great help for the DSC researchers. The results of this study imply that using TiO_2 powders of a large commercial batch instead of TiO_2 particles of homemade small different batches result in a more reproducible cell efficiency. This methodological investigation can contribute not only to the research of DSC, but also to various applications of industrial and scientific works in several fields as suggested in the introduction.

Acknowledgements

We acknowledge financial support of this work by the Swiss Science Foundation and Swiss Federal Office for Energy (OFEN). Peter Chen thanks the Taiwan Merit Scholarships Program (TMS-094-2A-026). The SEM-image works were carried out in the CIME of EPFL.

REFERENCES

1. O'Regan B, Grätzel M. A low cost, high-efficiency solar cell based on dye-sensitized colloidal TiO_2 films. *Nature (London)* 1991; **353**: 737–739.
2. Grätzel M. Photoelectrochemical cells. *Nature (London)* 2001; **414**: 338–344.
3. Wang P, Zakeeruddin SM, Comte P, Charvet R, Humphry-Baker R, Gratzel M. Enhance the performance of dye-sensitized solar cells by co-grafting amphiphilic sensitizer and hexadecylmalonic acid on TiO_2 nanocrystals. *Journal of Physical Chemistry B* 2003; **107**: 14336–14341.
4. Ito S, Nazeeruddin MK, Liska P, Comte P, Charvet R, Péchy P, Jirousek M, Kay A, Zakeeruddin SM, Gratzel M. Photovoltaic characterization of dye-sensitized solar cells: effect of device masking on conversion efficiency. *Progress in Photovoltaics* 2006; **14**: 589–601.

DOI: 10.1002/pip

5. Nazeeruddin Md K, De Angelis F, Fantacci S, Selloni A, Viscardi G, Liska P, Ito S, Takeru B, Grätzel M. Combined experimental and DFT-TDDFT computational study of photoelectrochemical cell ruthenium sensitizers. *Journal of the American Chemical Society* 2005; **127**: 16835–16847.
6. Tsoukleris DS, Arabatzis IM, Chatzivasiloglou E, Kontos AI, Belessi V, Bernard MC, Falaras P. 2-Ethyl-1-hexanol based screen-printed titania thin films for dye-sensitized solar cells. *Solar Energy* 2005; **79**: 422–430.
7. Zhang D, Ito S, Wada Y, Kitamura T, Yanagida S. Nanocrystalline TiO_2 electrodes prepared by water-medium screen printing technique. *Chemistry Letters* 2001; **30**: 1042–1043.
8. Gupta TK, Cirignano LJ, Shah KS, Moy LP, Kelly DJ, Squillante MR, Entine G, Smestad GP. Screen-printed dye-sensitized large area nanocrystalline solar cell. *Material Research Society Symposium Proceedings* 2000; **581**: 653–658.
9. Ma T, Kida T, Akiyama M, Inoue K, Tsunematsu S, Yao K, Noma H, Abe E. Preparation and properties of nanostructured TiO_2 electrode by a polymer organic-medium screen-printing technique. *Electrochemistry Communications* 2003; **5**: 369–372.
10. Nazeeruddin MK, Zakeeruddin SM, Humphry-Baker R, Jirousek M, Liska P, Vlachopoulos N, Shklover V, Fischer CH, Grätzel M. Acid-base equilibria of (2,2'-Bipyridyl-4,4'-dicarboxylic acid)ruthenium(II) complexes and the effect of protonation on charge-transfer sensitization of nanocrystalline titania. *Inorganic Chemistry* 1999; **38**: 6298–6305.
11. Bonhôte P, Dias AP, Armand M, Papageorgiou N, Kalyanasundaram K, Grätzel M. Hydrophobic, highly conductive ambient-temperature molten salts. *Inorganic Chemistry* 1996; **35**: 1168–1178.
12. Rothenberger G, Comte P, Grätzel M. A contribution to the optical design of dye-sensitized nanocrystalline solar cells. *Solar Energy Materials and Solar Cells* 1999; **58**: 321–336.
13. Tachibana Y, Hara K, Sayama K, Arakawa H. Quantitative analysis of light-harvesting efficiency and electron-transfer yield in ruthenium-dye-sensitized nanocrystalline TiO_2 solar cells. *Chemistry of Materials* 2002; **14**: 2527–2535.
14. Ito S, Yoshida S, Watanabe T. Preparation of Colloidal Anatase TiO_2 Secondary Submicroparticles by Hydrothermal Sol-Gel Method. *Chemistry Letters* 2000; **29**: 70–71.

DOI: 10.1002/pip